Ionically Self-Assembled, Multi-Luminophore One-Dimensional Micro- and Nanoscale Aggregates of Thiacarbocyanine GUMBOS

ARTICLE *in* THE JOURNAL OF PHYSICAL CHEMISTRY C · APRIL 2012

Impact Factor: 4.77 · DOI: 10.1021/jp3007848 · Source: PubMed

10 AUTHORS, INCLUDING:

Susmita Das
Louisiana State University
34 PUBLICATIONS **348** CITATIONS
SEE PROFILE

Bilal El-Zahab
Massachusetts Institute of Technology
49 PUBLICATIONS **729** CITATIONS
SEE PROFILE

Gary A Baker
University of Missouri
246 PUBLICATIONS **8,797** CITATIONS
SEE PROFILE

Isiah Warner
Louisiana State University
388 PUBLICATIONS **8,181** CITATIONS
SEE PROFILE

THE JOURNAL OF PHYSICAL CHEMISTRY C

Article

pubs.acs.org/JPCC

Ionically Self-Assembled, Multi-Luminophore One-Dimensional Micro- and Nanoscale Aggregates of Thiacarbocyanine GUMBOS

Sergio L. de Rooy,[†] Susmita Das,[†] Min Li,[†] Bilal El-Zahab,[†] Atiya Jordan,[†] Ridgely Lodes,[†] Anna Weber,[‡] Lin Chandler,[§] Gary A. Baker,[∥] and Isiah M. Warner*[,†]

[†]Department of Chemistry, Louisiana State University, Baton Rouge, Louisiana 70803, United States

[‡]Department of Chemistry, Marquette University, Milwaukee, Wisconsin 53201, United States

[§]Horiba Jobin Yvon Inc., Edison, 3880 Park Avenue, Edison, New Jersey 08820, United States

[∥]Department of Chemistry, University of Missouri, Columbia, Missouri 65211, United States

Supporting Information

ABSTRACT: Groups of uniform materials based on organic salts (GUMBOS), derived from thiacarbocyanine (TC)-based dyes with increasing methyne chain lengths, were prepared through a single-step metathesis reaction between the iodide form of the TC dye and lithium bis(perfluoroethylsulfonyl)imide as the lipophilic anion source. Ionic self-assembly of these fluorescent hydrophobic GUMBOS resulted in aqueous dispersions of one-dimensional micro- and nanoscale molecular aggregates. Blended binary and ternary aggregates containing multiple TC GUMBOS were also prepared. These nanostructures exhibited a variety of aspect ratios, affording tunable Förster resonance energy transfer (FRET) and aggregation-dependent spectroscopic properties.

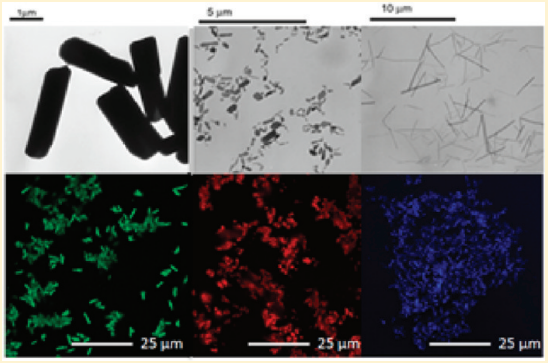

1. INTRODUCTION

Nanoscale aggregates of organic materials have gained widespread attention in fields such as biomedicine and optoelectronics due to the versatility and tunability of the electronic and photophysical properties of these materials.[1] The impact of such materials in these fields and others is expected to grow with new developments such as thin organic films in energy harvesting and in solid-state laser technology.[2] In the present work we examine dye aggregation within molecular aggregates, specifically thiacarbocyanines. We refer to these aggregates as molecular micro- and nanoscale aggregates to specify that their dimensions are either several micrometers or below 100 nm. One-dimensional nanomaterials are defined as those structures in which only one dimension is confined to the nanoscale, i.e., wires, rods, and tubes.[3]

Scheme 1. Thiacarbocyanine GUMBOS

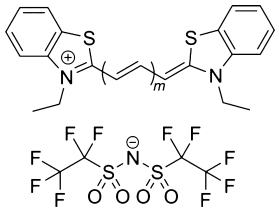

***m* = 0 [TCO][BETI]**
***m* = 1 [TC1][BETI]**
***m* = 2 [TC2][BETI]**

Fluorescent one-dimensional (1-D) nanomaterials have been the subject of considerable research over the past few years due to their potential use in fields such as nanoelectronics, energy harvesting, and bioimaging.[4] Designing such nanostructures has been achieved through various templated and nontemplated approaches. Fabrication of nanomaterials with desired morphologies and properties through spontaneous molecular self-assembly is particularly desirable, since such strategies require neither the use of additives nor templates.

Arrangement of organic dyes into extended supramolecular arrays is a well-established area and is usually recognized as the result of oriented dye aggregation, arising from various dispersive forces such as $\pi-\pi$, cation$-\pi$, electrostatic, ion–dipole, hydrophobic, and hydrogen bonding interactions between individual dye molecules.[5] As a result, coupled optical transitions often occur, leading to the formation of a diversity of aggregates, each with unique spectral properties. Dye aggregates are classified on the basis of type or directionality of intermolecular stacking. Head-to-tail molecular stacking is characterized by a narrow, bathochromically shifted (red-shifted) absorption band as compared to the monomeric dye and these aggregates are referred to as J-aggregates. Such J-

Received: January 24, 2012
Revised: February 16, 2012
Published: March 8, 2012

   dx.doi.org/10.1021/jp3007848 | *J. Phys. Chem. C* 2012, 116, 8251–8260

aggregates typically exhibit a small Stokes shift and enhanced fluorescence with fluorescence lifetimes shorter than the corresponding monomeric species.[6] Dye aggregates formed through a "card-pack" type of intermolecular stacking are characterized by a hypsochromically shifted (blue-shifted) broad absorption and are referred to as H-aggregates. These aggregates exhibit a large Stokes shift and strongly quenched fluorescence.[7] Both aggregation types have been well explained by Kasha[8] and Davydov.[9] It is also well established that J- and H-aggregations are influenced by environmental factors such as dye concentration, pH, temperature, salts, surfactants, and (poly)electrolytes, accordingly offering numerous pathways for tailoring.[10] The study of dye aggregation has led to seminal developments in a wide range of areas including molecular imaging,[11] photodynamic therapy,[12] polarizing and nonlinear optics,[13] laser technology,[14] and dye-sensitized solar cells.[15]

Cyanines, a family of versatile dyes which were initially used in the photographic industry, have received particular attention in the study of dye aggregation. Their aggregation behavior has been investigated in solution[16] as well as in thin films,[17] hybrid organoclays,[18] and electrospun fibers.[10] To date, however, there have only been a handful of reports on the synthesis and application of nanomaterials containing cyanine dyess.[19]

Our group has recently reported on a class of polyionic nanomaterials we have come to refer to as "groups of uniform materials based on organic salts", or hereafter simply "GUMBOS".[20] These GUMBOS are designer salts comprising bulky organic ions arranged in a disordered ionic lattice and have melting points that typically fall between room temperature and 250 °C. Being a solid-state analogue of ionic liquids, the physicochemical and functional properties of GUMBOS can be tailored through the appropriate selection of their respective cations and anions. A variety of these materials have been prepared with fluorescent, magnetic, and tumor-targeting properties.[20b,21] One of our studies demonstrated the preparation of near-infrared (NIR) fluorescent GUMBOS by ion-pairing a commercially available cationic cyanine dye with one of the various hydrophobic anions.[20c] Nanoparticles prepared from these NIR compounds showed illustrative potential as contrast agents for labeling monkey kidney fibroblast (Vero) cells. In another study, the aggregation and corresponding spectral properties of the NIR organic salts were systematically tailored by simply selecting from a variety of different hydrophobic anions.[20d] More recently, we reported on a templated method for the preparation of 1D nanostructures from rhodamine-based GUMBOS.[22]

The current study provides a facile route to examples of 1D nano- and microscale morphologies derived from a series of thiacarbocyanine (TC)-based GUMBOS (Scheme 1) with distinctive and attractive photoluminescent features. Nanomaterials derived from a series of thiacyanine iodide dyes bearing different alkyl side-chain lengths have been previously reported. In one particular study by Takazawa, dye molecules were dissolved in water at elevated temperature, allowing for self-assembly into nanowires under controlled-cooling conditions.[19a] In a later study from the same author, microrings were obtained through surface-assisted self-assembly of similar dyes.[19b] The resulting thiacyanine nanowires and microrings exhibited interesting optical waveguide properties, allowing them to function as suitable candidates for signal transduction in microelectronics devices. In another study, nanoparticles were prepared from a thiatricarbocyanine iodide dye using a reprecipitation approach in a variety of nonsolvents to yield nanoparticles of various shapes and sizes.[23]

Unlike dye aggregates which are typically encountered in solution at concentrations in the millimolar range, the nano- and microsized aggregates discussed here are formed in water at low micromolar concentrations. Thus, these concentrations are significantly lower than those typically observed for formation of aggregates. The micro- and nanoscale aggregates reported herein are obtained in solution as they are formed by reprecipitation, after rapidly injecting a small amount of TC dissolved in a dissoluting solvent into a nonsolvent. This study reports a straightforward anion-exchange procedure for synthesizing TC-based GUMBOS characterized by different spectral properties. The overall morphology of micro- and nanoscale structures subsequently obtained via room temperature reprecipitation[24] was dependent upon the particular TC dye chosen. Notably, the [BETI$^-$] anion was selected to impart pronounced hydrophobicity to the GUMBOS as compared to their iodide counterpart, facilitating the formation of ionically self-assembled[25] micro- and nanoscale aggregates in water at a 10^3-fold lower dye concentration (i.e, 2 μM) than reported previously. Studies employing transmission and scanning electron microscopy (TEM and SEM, respectively) imaging reveal that varying the methyne chain lengths exerts profound influence over the relative dimensions of the aggregates formed. Multiluminophore aggregates consisting of blends of two or three different TC species were prepared and found to exhibit different types of dye aggregation (J-, H-, and random) and Förster resonance energy transfer (FRET) between dyes within the aggregates. To the best of our knowledge, this represents the first example clearly illustrating FRET based on organic nanomaterials derived wholly from structural analogues of the same parent dye. These nano- and microscale blends with their unique and highly tunable spectral properties represent promising candidates for applications in areas including optoelectronics, bioimaging, energy harvesting, and biochemical sensing.

2. EXPERIMENTAL SECTION

2.1. Chemicals. The thiacarbocyanine (TC) dyes 3,3′-diethylthiacyanine iodide ([TC0][I]), 3,3′-diethylthiacarbocyanine iodide ([TC1][I]), and 3,3′-diethylthiadicarbocyanine iodide ([TC2][I]), as well as the deuterated solvents chloroform-d_1 and dimethyl sulfoxide-d_6, were purchased from Sigma-Aldrich (Milwaukee, WI). HPLC grade organic solvents, including acetonitrile, tetrahydrofuran, ethanol, methanol, and dichloromethane, were acquired from J.T. Baker (Philipsburg, NJ). Triply deionized ultrapure water (18.2 MΩ cm) was obtained using an Elga model PURELAB ultrapure water filtration system. Lithium bis-(pentafluoroethane)sulfonimide salt was a generous gift from 3M. All reagents were used without further purification.

Table 1. Overlap Integrals ($J(\lambda)$) and Energy Transfer Efficiencies (E) of Various TC Donor (D)−Acceptor (A) Pairs

D−A pair	$J(\lambda)$	E
TC01	2.07×10^{-13}	30.3%
TC12	2.78×10^{-13}	49.1%
TC02	9.56×10^{-14}	30.2%
TC012		45.0%, 61.4%

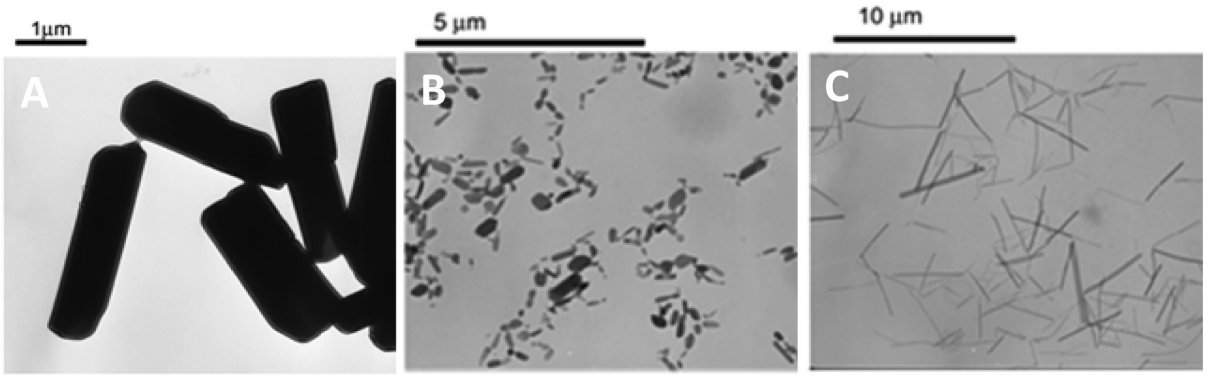

Figure 1. TEM micrographs of (A) [TC0][BETI], (B) [TC1][BETI], and (C) [TC2][BETI] aggregates.

2.2. Synthesis and Characterization. The TC GUMBOS were prepared utilizing a metathesis reaction between thiacarbocyanine iodides and lithium bis(pentafluoroethane)-sulfonimide at a molar ratio of 1 to 1.1. The reaction was performed in a biphasic mixture of water and dichloromethane (1:5, v/v) under stirring for 24 h. Afterward, the organic phase containing the TC GUMBOS was washed several times with distilled water to remove residual LiI byproduct. Finally, the GUMBOS were isolated by solvent removal using rotary evaporation.

These TC-based salts were characterized with nuclear magnetic resonance (H^1-, C^{13}-, and F^{19}-NMR) and high-resolution mass spectrometry (HR-MS). The results are shown in Figures S1 and S2 in the Supporting Information, respectively. H^1- and C^{13}-NMR spectra of the GUMBOS revealed peaks similar to those of the thiacarbocyanine iodide parent compound, confirming the presence of [TC^+] cations after ion-exchange. Two peaks were observed in F^{19}-NMR spectra, with chemical shifts of −78.9 and −117.7 Hz, both of which are characteristic of the presence of the [$BETI^-$] anion. Additional characterization was performed using HR-MS on an Agilent 6210 electrospray ionization time-of-flight instrument. In positive-ion mode, intense peaks with m/z of 339.10, 365.13, and 391.14 were observed, corresponding to molecular weights for the [$TC0^+$], [$TC1^+$], and [$TC2^+$] cation, respectively. In negative-ion mode, a peak was observed at 379.91 m/z characteristic of the [$BETI^-$] anion.

2.3. Preparation of TC-Based Micro- and Nanostructures. The TC-based micro- and nanoscale molecular aggregates were prepared using a well-known reprecipitation method at room temperature.[26] In brief, ethanolic solutions at a GUMBOS concentration of 0.1 mM were prepared and 100 μL aliquots were added to 5 mL of distilled water under sonication (BRANSON 3510RDTH model bath ultrasonicator, 335 W, 40 kHz frequency) for 5 min. The resulting solutions were left to equilibrate for 10 min. As a result, 1-D micro- or nanoscale aggregates were formed from an initial dye concentration of 2 μM, with each TC dye yielding a unique morphology with its associated spectral properties as evidenced by electron microscopy and spectral analysis.

Blended nanoscale molecular aggregates containing multiple TC luminophores were similarly prepared from mixtures of ethanolic stocks consisting of the desired TC GUMBOS. By our nomenclature, [TC01][BETI] denotes GUMBOS formed from a precursor solution of [$TC0^+$] and [$TC1^+$] subjected to the reprecipitation process, [TC02][BETI] is formed from [$TC0^+$] and [$TC2^+$], and so on. The molar ratios of TC precursor solutions (0.1 mM) were varied to examine the effect of concentration on the spectral properties and morphologies of blended nanostructures. Thus, binary materials with molar ratios of 1:100, 10:100, 100:100, 100:10, and 100:1, respectively were prepared, where 100 and 1 represent concentrations of 2 and 0.02 μM for the initial TC dye concentration in the aggregate. Similarly, molar ratios of 100:10:10, 10:100:10, 10:10:100, and 100:100:100 for each TC GUMBOS were employed for the ternary blend [TC012]-[BETI]. TEM images of the binary and ternary nanostructures are provided in Figure 3.

2.4. Optical Spectroscopy. The spectral properties of these TC-based micro- and nanosized self-assemblies were investigated by use of absorbance and fluorescence spectroscopies. Absorbance measurements were performed on a Shimadzu UV-3101PC UV−vis−NIR scanning spectrometer (Shimadzu, Columbia, MD). Fluorescence emission was collected using a Spex Fluorolog-3 spectrofluorimeter (model FL3-22TAU3; Jobin-Yvon, Edison, NJ). Both fluorescence and absorbance were acquired using a 0.4 cm^3 quartz cuvette (Starna Cells) and water as the blank.

2.5. Lifetime Instrumentation. Fluorescence lifetime measurements were performed at Horiba Jobin Yvon, NJ, using the time domain mode. Picosecond pulsed excitation sources of 408 and 495 nm were used, respectively, with a TBX detector. Data acquisition was carried out using time-correlated single-photon counting (TSCPC) mode with a resolution of 7 ps/channel.

2.6. Calculations of Förster Resonance Energy Transfer (FRET) Parameters. The spectral overlap integrals for the various TC pairs were calculated using the formula

$$J(\lambda) = \int_0^\infty \varepsilon(\lambda) f(\lambda) \lambda^4 \, d\lambda \quad (1)$$

where $J(\lambda)$ is the overlap integral, ε is the extinction coefficient of the acceptor, f is the normalized emission spectrum of the donor, and λ is the wavelength. The energy transfer efficiencies were calculated on the basis of the formula

$$E = 1 - \frac{F_{DA}}{F_D} \quad (2)$$

where F_{DA} and F_D represent the integrated fluorescence intensity of the donor in the presence and absence of acceptor, respectively.[27] The $J(\lambda)$ and E values are compiled in Table 1.

2.7. Electron and Fluorescence Microscopy. Electron microscopy images of the TC-based nanostructures were captured using an SM-6610, JSM-6610LV high- and low-

dx.doi.org/10.1021/jp3007848 | J. Phys. Chem. C 2012, 116, 8251−8260

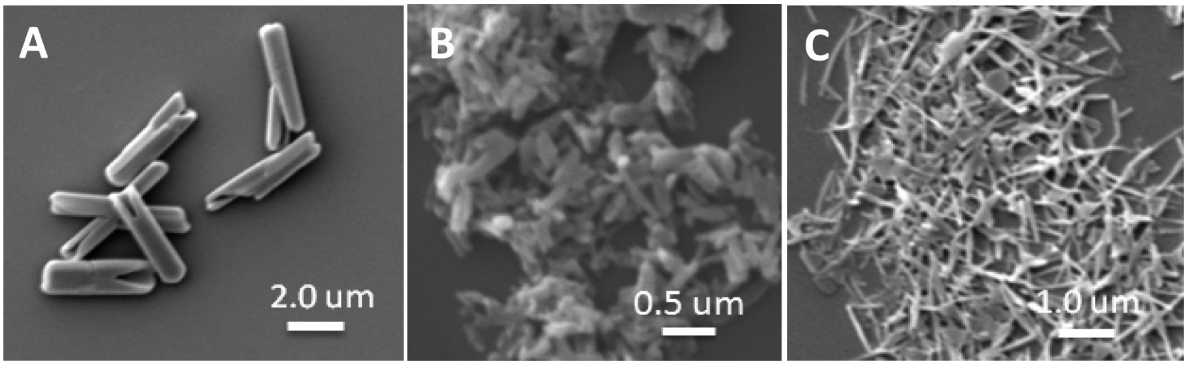

Figure 2. SEM micrographs of (A) [TC0][BETI], (B) [TC1][BETI], and (C) [TC2][BETI] aggregates.

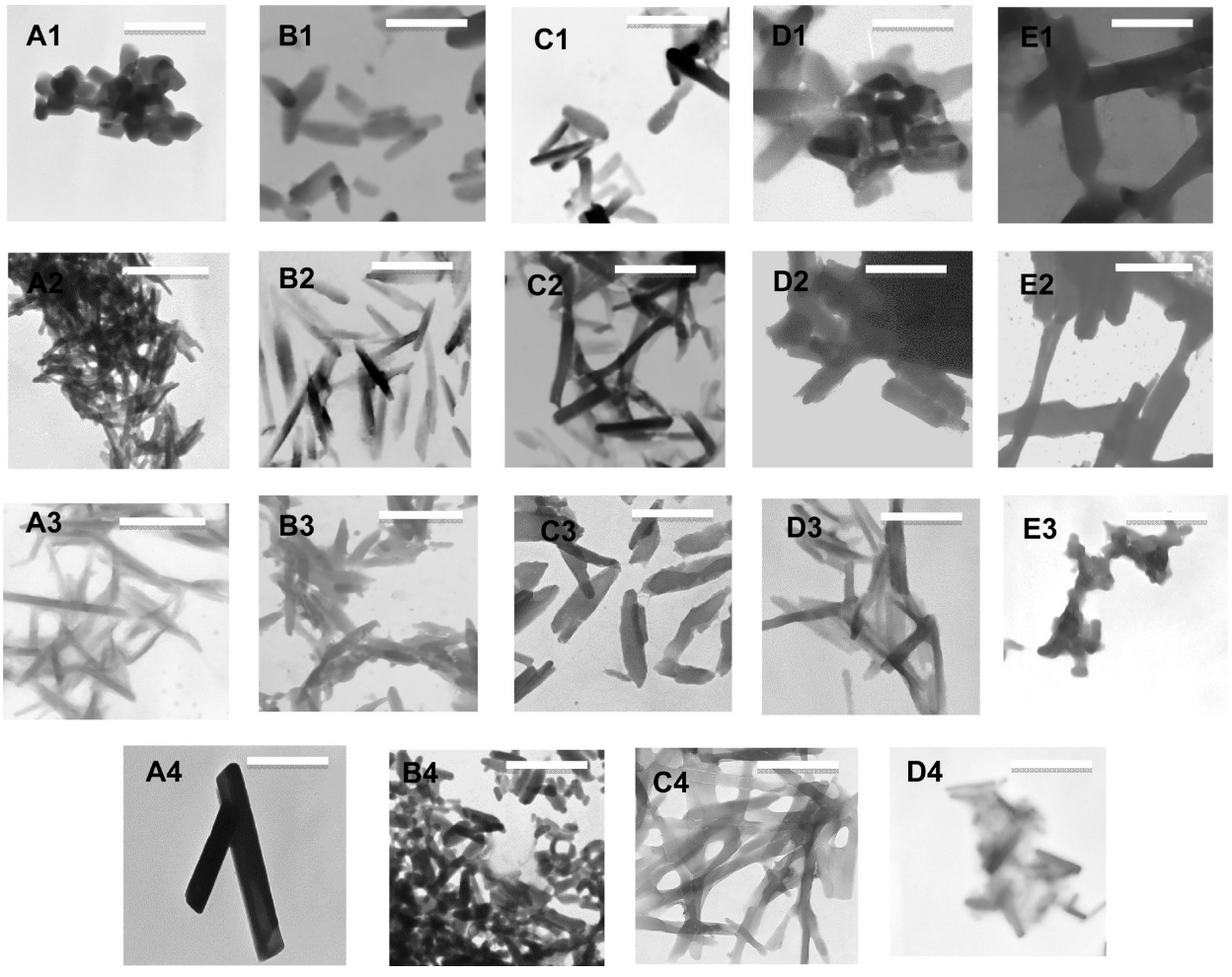

Figure 3. TEM micrographs of blended TC nanoscale aggregates of (A1–E1) [TC01][BETI], (A2–E2) [TC02][BETI], and (A3–E3) [TC12][BETI] at molar ratios of 1:100, 10:100, 100:100, 100:10, and 100:1, respectively, and (A4–E4) [TC012][BETI] at ratios of 100:10:10, 10:100:10, 10:10:100, and 100:100:100. The scale bar represents 1 μm.

vacuum scanning electron microscope (SEM) and a JEOL 100CX transmission electron microscope (TEM). Fluorescence images were obtained using a Leica TCS SP2 scanning laser confocal system with a 63× NA 1.4 lens. Images (1024 × 1024 pixels) were acquired on the basis of six averages.

3. RESULTS AND DISCUSSION

3.1. Characterization of TC-Based Micro- and Nanostructures. Electron microscopy (TEM and SEM) images of the TC micro- and nanoscale molecular aggregates obtained via reprecipitation are shown in Figures 1 and 2, respectively. Rodlike [TC0][BETI] aggregates with diameters of 0.82 ± 0.13 μm and lengths of 2.42 ± 0.20 μm, for an aspect ratio near 3, were found. Close examination of the SEM images of Figure 2 reveals that some of these aggregates exhibit semitubular features. In the case of [TC1][BETI], the aspect ratios of the aggregates vary widely, exhibiting both rod and wirelike morphologies with diameters of 153 ± 74 nm and lengths of 0.53 ± 0.16 μm. Finally, well-defined [TC2][BETI] wire-

dx.doi.org/10.1021/jp3007848 | J. Phys. Chem. C 2012, 116, 8251–8260

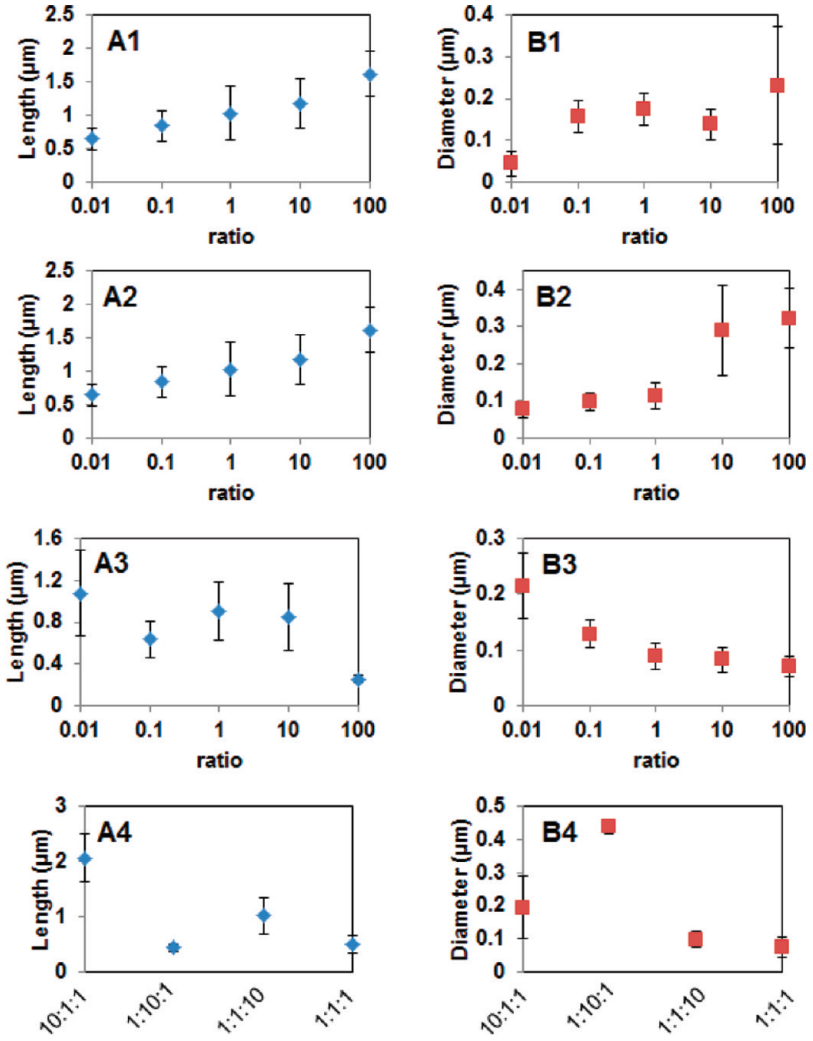

Figure 4. Length (A) and diameter (B) of nanoscale aggregates at different molar ratios: (1) [TC01][BETI], (2) [TC02][BETI], (3) [TC12][BETI], and (4) [TC012][BETI].

shaped aggregates are obtained with diameters of 137 ± 37 nm and lengths of 3.16 ± 1.13 μm.

TC-based GUMBOS with different anions such as [BF_4^-], [PF_6^-], and tetraphenylborate ([TPB^-]) were prepared as controls. In contrast to the [$BETI^-$]-based GUMBOS, these compounds failed to self-assemble into either defined 1-D aggregates or any specific morphology for that matter. Thus, the formation of micro- and nanoscale aggregates is clearly linked to a unique and favorable association between [TC^+] cations and [$BETI^-$] counterions. A further series of control experiments performed using the iodide precursors of the TC dyes (i.e., [TC0][I], [TC1][I], [TC2][I]) revealed that only [TC0][I] yielded 1-D nanoscale aggregates upon reprecipitation. We note that the final solution concentration of [TC0][I] used in this experiment was 3 orders of magnitude lower than previous reports on the preparation of nanowires from similar dyes.[19a] The TC-based molecular aggregates reported in this work have another distinct advantage in that they can be prepared at room temperature in only a handful of minutes employing a very simple and general reprecipitation approach.

3.2. Spectral Properties of TC-Based Micro- and Nanostructures. The absorbance properties of the TC materials were measured at dye concentrations equivalent to 2 μM in water. On the basis of solution electronic absorption measurements, the maximum absorbance wavelengths for [TC0][BETI], [TC1][BETI], and [TC2][BETI] structures were 423, 557, and 649 nm, respectively, consistent with the increased conjugation across the series (Figure 3). In addition to the absorption maximum, [TC1][BETI] aggregates exhibited a red-shifted peak at 631 nm representative of J aggregation. An additional blue-shifted peak was observed at 475 nm for the [TC2][BETI] spectrum, characteristic of H aggregation. Fluorescence spectroscopic measurements were also performed for the TC nanostructures. Dispersions of [$TC0^+$], [$TC1^+$], and [$TC2^+$] aggregates were excited at 423, 541, and 644 nm, respectively. Their corresponding emission maxima were recorded at 464, 564, and 664 nm (Figure 5).

In addition to spectroscopic analysis, dispersions of TC-based micro- and nanoscale aggregates were also investigated using fluorescence microscopy. [TC0][BETI] microparticles excited using a 488 nm argon-ion laser line yielded strong emission in the green, as shown in Figure 6a. Likewise, [TC1][BETI] nanowires and rods excited by a 543 nm laser displayed red luminescence (Figure 6b). In the case of [TC2][BETI], the nanowires were excited using a 633 nm laser and imaged in the NIR (650−750 nm). A false-colored image of these nanostructures is given in Figure 6c. It should be noted that these various nanoscale aggregates exhibited bright,

dx.doi.org/10.1021/jp3007848 | J. Phys. Chem. C 2012, 116, 8251−8260

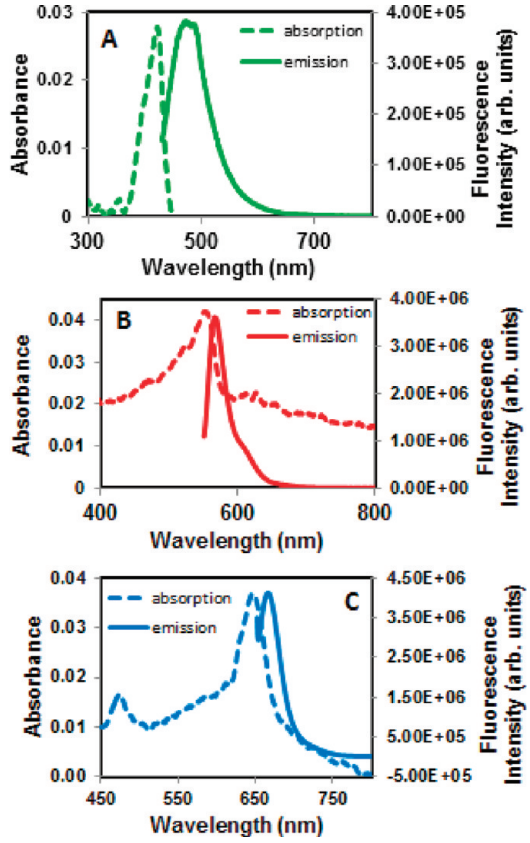

Figure 5. Normalized UV−vis and fluorescence emission spectra of nanoscale aggregates of (A) [TC0][BETI], (B) [TC1][BETI], and (C) [TC2][BETI]. Fluorescence excitation at 423 nm ($[TC0]_0$ = 2 μM), 541 nm ($[TC1]_0$ = 2 μM), and 644 nm ($[TC2]_0$ = 2 μM), respectively.

dye-specific fluorescence, suggesting possible avenues in multicolor imaging.

3.3. Binary and Ternary TC-Based Nanostructures. Biomimetic photosystems of cyanine triads have been previously reported.[28] Oppositely charged polyelectrolytes that self-assembled into capsules served as templates to which negatively charged thiacyanine dyes could adhere, allowing for FRET to occur between the exterior and interior of the capsule.

In the present study, molecular aggregates from TC blends were prepared by coprecipitation of a mixture of TC GUMBOS, resulting in structures containing multiple TC dyes, making the prospect of FRET an intriguing possibility. Verification for the formation of intimately blended nanostructures was evidenced through examination of TEM images with comparison to physical mixtures of preformed aggregates prepared from the individual TCs. Dual- and multiluminophore aggregates possessing different morphologies and spectral features were observed in the case where a dye mixture is subjected to reprecipitation conditions.

3.3.1. Electron Microscopy Studies. TEM micrographs were obtained of the blended binary and ternary nanomaterials for different molar ratios (Figure 3). Interestingly, the morphologies of the nanostructures appeared to be highly dependent on the concentrations of TC dyes; i.e., higher ratios of [TC0$^+$] resulted in increasing lengths and diameters of the aggregates, similar to [TC0][BETI] microstructures. Likewise, higher ratios of [TC1$^+$] lead to decreasing length and diameter of the structures, as was the case with [TC1][BETI] nanostructures. The corresponding lengths and diameters of the blended nanostructures at different dye ratios are depicted in Figure 4.

3.3.2. Absorption Spectroscopy Studies. Absorption spectra for binary ([TC01][BETI], [TC02][BETI], [TC12][BETI]) and ternary ([TC012][BETI]) nanostructures were obtained at various molar ratios of individual fluorophores. The respective absorption spectra are provided in Figure 7. These data clearly indicate that the absorption features of the individual TC-based dyes are retained within the blended nanostructures with the appearance of additional peaks in some cases. For example, [TC01][BETI] exhibits two monomer peaks of the parent TC dyes at 423 and 557 nm, respectively. At higher molar concentrations of [TC1$^+$] (100), a red-shifted peak corresponding to J aggregation was also observed at 631 nm. For [TC02][BETI], the monomer peaks of [TC0$^+$] and [TC2$^+$] were observed at 423 and 649 nm, respectively. In addition, two blue-shifted peaks were observed for [TC2$^+$] at 475 and 567 nm which are indicative of H aggregation. The peak observed at 475 nm appeared to be relatively sharp, suggesting a possible twisted H aggregation. For [TC12][BETI], the monomer peaks of [TC1$^+$] and [TC2$^+$] were observed at 557 and 649 nm, respectively. H aggregation was observed for [TC2$^+$] with a distinctive red-shifted peak at 475 nm appearing at higher molar ratios of this species (100). Interestingly, J aggregation was also observed at certain molar ratios. A characteristic peak at 753 nm was observed for molar ratios of 100:100 and 100:10 between [TC1$^+$] and [TC2$^+$]. [TC012][BETI] exhibits a

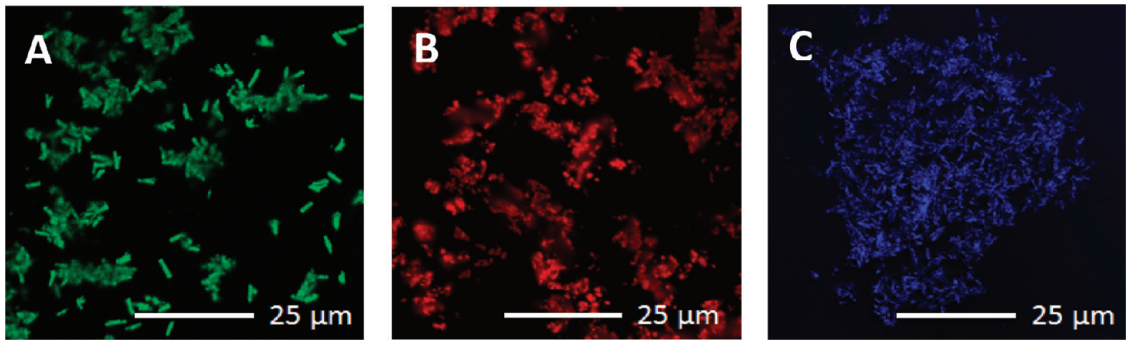

Figure 6. Fluorescence micrographs of (A) [TC0][BETI] aggregates (excitation was performed with a ArKr laser at 488 nm, and emission was collected between 500 and 578 nm), (B) [TC1][BETI] aggregates (excitation was performed with a green HeNe laser at 543 nm, and emission was collected between 555 and 700 nm), and (C) [TC2][BETI] aggregates (excitation was performed with a HeNe laser at 633 nm with emission collected between 650 and 750 nm). Images were pseudocolored blue in order to distinguish them from the [TC1][BETI] aggregates.

dx.doi.org/10.1021/jp3007848 | J. Phys. Chem. C 2012, 116, 8251−8260

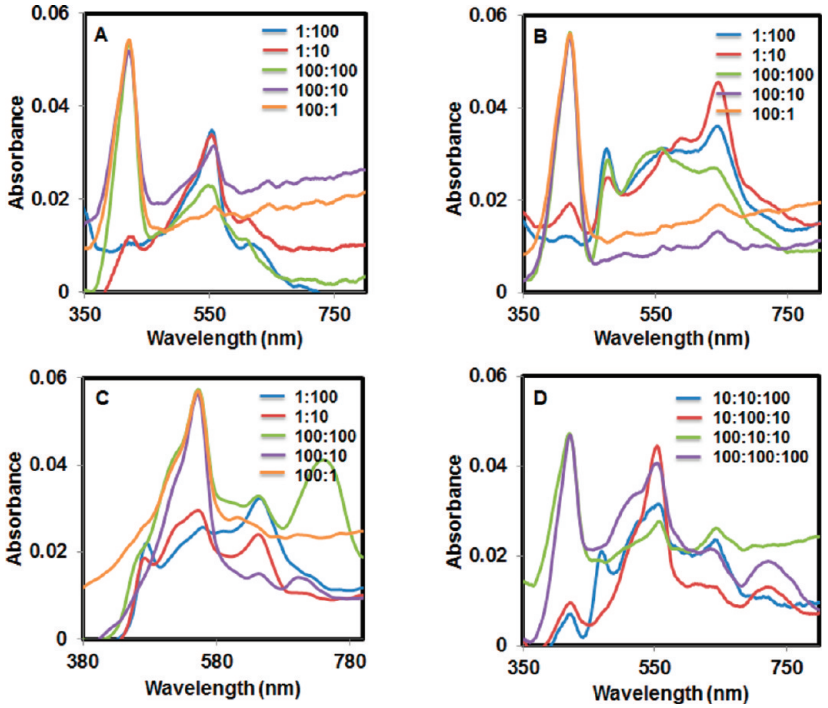

Figure 7. Normalized UV−vis spectra of binary (A) [TC01][BETI], (B) [TC02][BETI], (C) [TC12][BETI], and ternary aggregates (D) [TC012][BETI] at different molar ratios.

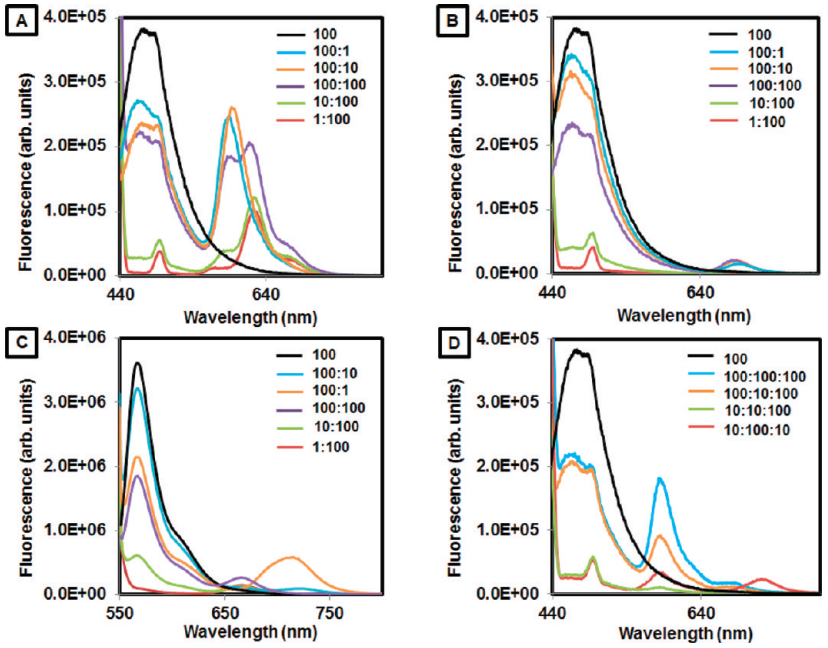

Figure 8. Fluorescence spectra of (A) [TC01][BETI], (B) [TC02][BETI], (C) [TC12][BETI], and (D) [TC012][BETI] binary and ternary aggregates at different molar ratios.

complex absorption profile containing features representative of the individual TC-based species. Similar to [TC12][BETI], J aggregation was also observed for [TC012][BETI] at molar ratios of 100:100 and 100:10.

3.3.2. Fluorescence Spectroscopy Studies. Fluorescence spectroscopy was used to study the spectral properties and examine the possibility of FRET within the binary as well as the ternary TC-based nanostructures. The emission spectra for these blended TC aggregates are shown in Figure 8. The most pronounced decrease in donor fluorescence was observed at higher molar ratios of donor and acceptor species. The overlap integral, $J(\lambda)$, and energy transfer efficiencies, E, for these blended TC nanostructures in water were calculated using eqs 1 and 2, respectively, and are found in Table 1.

It appears from these calculations that the $J(\lambda)$ value for [TC12][BETI] is the highest, followed by the value determined for [TC01][BETI] which is itself over twice that in [TC02][BETI]. The energy transfer efficiency for [TC12]-[BETI] is also the highest in the binary blends at roughly 49%. Interestingly, the fluorescence yield of the acceptor following

dx.doi.org/10.1021/jp3007848 | J. Phys. Chem. C 2012, 116, 8251−8260

Table 2. Recovered Intensity Decay Parameters for Single- and Multi-Luminophore Micro- and Nanoscale Aggregates Based on TC Parent Ion Structures

	lifetime	pre-exponential factor	amplitude	average lifetime	χ^2
[TC0] [BETI]	τ_1 = 681 ps	47% (J)	27%	1.19 ns	1.08
	τ_2 = 1.55 ns	52% (M)	68%		
	τ_3 = 5.14 ns	1%	5%		
[TC1] [BETI]	τ_1 = 158 ps	96% (J)	80%	167 ps	1.03
	τ_2 = 7.59 ns	3% (M)	15%		
	τ_3 = 2.37 ns	1%	5%		
[TC01] [BETI]	τ_1 = 135 ps	96%	67%	191 ps	1.30
	τ_2 = 1.07 ns	4%	22%		
	τ_3 = 4.34 ns	<1%	11%		
[TC02] [BETI]	τ_1 = 104 ps	99%	81%	128 ps	1.27
	τ_2 = 1.19 ns	1%	12%		
	τ_3 = 5.3 ns	<1%	7%		
[TC012] [BETI]	τ_1 = 75 ps	99%	82%	92 ps	1.25
	τ_2 = 1.46 ns	1%	10%		
	τ_3 = 5.83 ns	<1%	8%		

excitation of the donor is found to be enhanced in some cases while remaining unaffected in other systems. For instance, in the case of [TC01][BETI], [TC02][BETI], and [TC012]-[BETI], it was observed that, upon excitation of the [TC0$^+$] donor, the donor fluorescence decreased with respect to the pure donor concomitant with an enhanced acceptor emission relative to the lone acceptor, predictable FRET behavior. In [TC01][BETI], two peaks were observed for the acceptor at a molar ratio of 100:100 for the individual TC dyes. The peak at 583 nm is believed to be that of the monomer species, while the second at 613 nm is associated with J aggregation. As the relative concentration of the donor species [TC0$^+$] is reduced (10:100 and 1:100), the intensity of the acceptor monomer species [TC1$^+$] decreases significantly, while that of the J aggregate is still present upon excitation of the donor. This finding suggests that the fluorescence emission around 583 nm is the result of FRET between [TC0$^+$] and [TC1$^+$]. Alternatively, higher fluorescence intensity is recorded for the acceptor monomer species when the relative concentration of this species is reduced (100:1 and 100:10). It seems FRET is no longer distributed evenly between the acceptor monomer species and the J aggregate; rather, it is restricted to the monomer species. As a result, an increase in fluorescence intensity at 583 nm for the monomer peak is observed.

In [TC02][BETI], FRET was observed at higher relative concentrations of the donor species [TC0$^+$] (100). At lower concentrations of [TC0$^+$], energy transfer was not observed. In comparison to [TC01][BETI], the observed FRET appeared to be lower at all ratios. These findings are believed to be the result of a smaller overlap integral (Table 1) and the occurrence of H aggregation in [TC2$^+$] at higher molar ratios. Therefore, the similar fluorescence intensity observed for [TC02][BETI] at a molar ratio of 100:10 and 100:100 can be attributed to the occurrence of these nonfluorescent H aggregates.

[TC12][BETI] exhibited maximum FRET for the 100:100 molar ratio with the most significant decrease in donor intensity and increase in acceptor intensity. There appeared to be no FRET between the monomer emission of [TC1$^+$] and the absorption of the J aggregate of [TC2$^+$] due to the absence of spectral overlap between both. The lower concentration of the acceptor (100:10) resulted in a reduced FRET, as can be seen in a decrease in energy transfer efficiency and intensity of the donor emission. Interestingly, for the molar ratio of 100:1, a red-shifted emission was recorded with high fluorescence intensity at 707 nm. This emission peak appears to be the result of FRET between the donor and acceptor species.

The ternary [TC012][BETI] system revealed significant energy transfer efficiency for higher concentrations of [TC0$^+$] at molar ratios of 100:100:100 and 100:10:10. FRET appeared to be more apparent in the former, where a higher intensity was recorded for the [TC1$^+$] species. Similarly, energy transfer from [TC1$^+$] to [TC2$^+$] appeared to be more prominent at this molar ratio (100:100:100). However, some H aggregation is believed to occur, limiting a drastic increase in acceptor fluorescence as was observed in [TC01][BETI]. When the [TC0$^+$] concentration was decreased, FRET from [TC0$^+$] to [TC1$^+$] was very low. At a molar ratio of 10:100:10, an additional red-shifted peak was observed at 712 nm, suggesting FRET between [TC1$^+$] and [TC2$^+$], similar to [TC12][BETI] (100:1).

Thus, it appears that FRET was found to occur within the binary and ternary blends and was favored at higher concentrations of TC species. In addition, nonfluorescent H-aggregates involving the acceptor within blended nanostructures appeared in [TC02][BETI] and [TC012][BETI], resulting in traps which open up additional nonradiative pathways of energy loss.

3.4. Fluorescence Lifetime Analysis. Binary and ternary TC-based nanostructures were further analyzed using fluorescence decay analysis. Excited-state decay data were analyzed in terms of a multiexponential decay model, and the recovered parameters are summarized in Table 2. Excited-state lifetimes were determined for structures consisting of single species ([TC0][BETI] and [TC1][BETI]) as well as multiple species ([TC01][BETI], [TC02][BETI], and [TC012][BETI]). In the case of [TC0][BETI], two discrete excited-state lifetimes were observed which we attribute to the approximately equal contributions from J-aggregates (681 ps, 47%) and monomeric species (1.55 ns, 52%). The [TC1][BETI] nanostructures exhibited a much shorter average lifetime resulting from the prevalence of J-aggregation (96%) which exhibited an apparent lifetime of 158 ps. Comparable lifetimes have been reported for thia(carbo)cyanines in other systems.[29] The lifetimes of the binary and ternary TC-based nanostructures were all similar to that in the [TC1][BETI] nanostructures. These results support our claim for the occurrence of FRET within these GUMBOS.

CONCLUSIONS

Thiacarbocyanine-based GUMBOS were successfully prepared through a facile anion-exchange reaction. The iono-hydrophobic properties of these materials facilitate a room temperature preparation of 1-D structures on the micrometer and nanoscale via a straightforward reprecipitation at ultradilute

dx.doi.org/10.1021/jp3007848 | J. Phys. Chem. C 2012, 116, 8251−8260

(i.e., micromolar) dye concentrations. The micro- and nanoscale molecular aggregates were rapidly obtained through spontaneous formation of ionic self-assemblies. Binary and ternary aggregates were similarly obtained by intimately mixing multiple TCs prior to initiating the reprecipitation. These materials exhibited tunable spectral properties as a result of efficient FRET, as well as changes in dye aggregation within the blended materials, which was most pronounced at higher molar ratios of the TCs. The highest energy transfer efficiency was obtained from [$TC1^+$] to [$TC2^+$]. Measurement of the fluorescence lifetimes of the binary and ternary nanoscale aggregates confirmed the stationary-state results, suggesting the occurrence of FRET. Further studies are being conducted to better understand and improve the FRET efficiency, aggregation-induced fluorescence changes in similar cyanine dye nanostructures, and multicolor multiluminophore aggregates. The TC-based aggregates reported here, and especially their tunable spectral properties, offer potential applications in optoelectronics, (bio)chemical sensing, and bioimaging.

■ ASSOCIATED CONTENT

Supporting Information

The synthetic yields, melting points, NMR spectra (^1H, ^{13}C, ^{19}F), and ESI-MS of TC-derived GUMBOS; PL quantum yields; TEM and fluorescence micrographs of GUMBOS nanoparticles. This material is available free of charge via the Internet at http://pubs.acs.org.

■ AUTHOR INFORMATION

Corresponding Author

*E-mail: iwarner@lsu.edu. Phone: (225) 578-2829. Fax: (225) 578-3971.

Notes

The authors declare no competing financial interest.

■ ACKNOWLEDGMENTS

The authors thank the National Science Foundation (CHE-0911118) and the National Institutes of Health (1R01GM079670) for generous funding as well as the American Chemical Society Division of Analytical Chemistry and Eli Lilly and Company for the graduate fellowship provided to S.L.d.R. The authors also thank Matthew Brown for help with fluorescence microscopy experiments and Vivian Fernand for technical assistance.

■ REFERENCES

(1) (a) Imahori, H.; Umeyama, T.; Ito, S. Large π-Aromatic Molecules as Potential Sensitizers for Highly Efficient Dye-Sensitized Solar Cells. *Acc. Chem. Res.* **2009**, *42* (11), 1809−1818. (b) Fernanda, R. Photophysical properties of porphyrins in biological membranes. *J. Photochem. Photobiol., B* **1995**, *29* (2−3), 109−118.

(2) (a) Sayama, K.; Tsukagoshi, S.; Mori, T.; Hara, K.; Ohga, Y.; Shinpou, A.; Abe, Y.; Suga, S.; Arakawa, H. Efficient sensitization of nanocrystalline TiO2 films with cyanine and merocyanine organic dyes. *Sol. Energy Mater. Sol. Cells* **2003**, *80* (1), 47−71. (b) Costela, A.; Garcia-Moreno, I.; Sastre, R. Polymeric solid-state dye lasers: Recent developments. *Phys. Chem. Chem. Phys.* **2003**, *5* (21), 4745−4763.

(3) Zang, L.; Che, Y.; Moore, J. S. One-Dimensional Self-Assembly of Planar pi-Conjugated Molecules: Adaptable Building Blocks for Organic Nanodevices. *Acc. Chem. Res.* **2008**, *41* (12), 1596−1608.

(4) Zhao, Y. S.; Fu, H. B.; Peng, A. D.; Ma, Y.; Liao, Q.; Yao, J. N. Construction and Optoelectronic Properties of Organic One-Dimensional Nanostructures. *Acc. Chem. Res.* **2010**, *43* (3), 409−418.

(5) Fabian, J.; Nakazumi, H.; Matsuoka, M. Near-Infrared Absorbing Dyes. *Chem. Rev.* **1992**, *92* (6), 1197−1226.

(6) (a) Jelley, E. E. Spectral absorption and fluorescence of dyes in the molecular state. *Nature* **1936**, *138*, 1009−1010. (b) Scheibe, G.; Rivas, A. A new method in quantitive emission spectral analysis adaptable also as a micro method. *Angew. Chem.* **1936**, *49*, 0443−0446.

(7) Eisfeld, A.; Briggs, J. S. The J- and H-bands of organic dye aggregates. *Chem. Phys.* **2006**, *324* (2−3), 376−384.

(8) Mcrae, E. G.; Kasha, M. Enhancement of Phosphorescence Ability Upon Aggregation of Dye Molecules. *J. Chem. Phys.* **1958**, *28* (4), 721−722.

(9) Davydov, A. S. *Theory of Molecular Excitons*; McGraw-Hill: New York, 1962.

(10) Demir, M. M.; Ozen, B.; Ozcelik, S. Formation of Pseudoisocyanine J-Aggregates in Poly(vinyl alcohol) Fibers by Electrospinning. *J. Phys. Chem. B* **2009**, *113* (34), 11568−11573.

(11) Advincula, R. C.; Fells, E.; Park, M. K. Molecularly ordered low molecular weight azobenzene dyes and polycation alternate multilayer films: Aggregation, layer order, and photoalignment. *Chem. Mater.* **2001**, *13* (9), 2870−2878.

(12) Kim, S.; Ohulchanskyy, T. Y.; Pudavar, H. E.; Pandey, R. K.; Prasad, P. N. Organically modified silica nanoparticles co-encapsulating photosensitizing drug and aggregation-enhanced two-photon absorbing fluorescent dye aggregates for two-photon photodynamic therapy. *J. Am. Chem. Soc.* **2007**, *129* (9), 2669−2675.

(13) (a) Wurthner, F.; Yao, S.; Debaerdemaeker, T.; Wortmann, R. Dimerization of merocyanine dyes. Structural and energetic characterization of dipolar dye aggregates and implications for nonlinear optical materials. *J. Am. Chem. Soc.* **2002**, *124* (32), 9431−9447. (b) Williams, D. J. Organic Polymeric and Non-Polymeric Materials with Large Optical Nonlinearities. *Angew. Chem., Int. Ed.* **1984**, *23* (9), 690−703.

(14) (a) Maeda, M. *Lasers Dyes*; Academic Press: Tokyo, 1984. (b) Rahn, M. D.; King, T. A. Comparison of laser performance of dye molecules in sol-gel, polycom, ormosil, and poly(methyl methacrylate) host media. *Appl. Opt.* **1995**, *34* (36), 8260−8271.

(15) Robertson, N. Optimizing dyes for dye-sensitized solar cells. *Angew. Chem., Int. Ed.* **2006**, *45* (15), 2338−2345.

(16) Khairutdinov, R. F.; Serpone, N. Photophysics of cyanine dyes: Subnanosecond relaxation dynamics in monomers, dimers, and H- and J-aggregates in solution. *J. Phys. Chem. B* **1997**, *101* (14), 2602−2610.

(17) Ariga, K.; Lvov, Y.; Kunitake, T. Assembling alternate dye-polyion molecular films by electrostatic layer-by-layer adsorption. *J. Am. Chem. Soc.* **1997**, *119* (9), 2224−2231.

(18) Eren, E.; Afsin, B. Investigation of a basic dye adsorption from aqueous solution onto raw and pre-treated bentonite surfaces. *Dyes Pigm.* **2008**, *76* (1), 220−225.

(19) (a) Takazawa, K.; Kitahama, Y.; Kimura, Y.; Kido, G. Optical waveguide self-assembled from organic dye molecules in solution. *Nano Lett.* **2005**, *5* (7), 1293−1296. (b) Takazawa, K. Micrometer-sized rings self-assembled from thiacyanine dye molecules and their waveguiding properties. *Chem. Mater.* **2007**, *19* (22), 5293−5301.

(20) (a) Tesfai, A.; El-Zahab, B.; Bwambok, D. K.; Baker, G. A.; Fakayode, S. O.; Lowry, M.; Warner, I. M. Controllable formation of ionic liquid micro- and nanoparticles via a melt-emulsion-quench approach. *Nano Lett.* **2008**, *8* (3), 897−901. (b) Tesfai, A.; El-Zahab, B.; Kelley, A. T.; Li, M.; Garno, J. C.; Baker, G. A.; Warner, I. M. Magnetic and Nonmagnetic Nanoparticles from a Group of Uniform Materials Based on Organic Salts. *ACS Nano* **2009**, *3* (10), 3244−3250. (c) Bwambok, D. K.; El-Zahab, B.; Challa, S. K.; Li, M.; Chandler, L.; Baker, G. A.; Warner, I. M. Near-Infrared Fluorescent NanoGUMBOS for Biomedical Imaging. *ACS Nano* **2009**, *3* (12), 3854−3860. (d) Das, S.; Bwambok, D.; Ei-Zahab, B.; Monk, J.; de Rooy, S. L.; Challa, S.; Li, M.; Hung, F. R.; Baker, G. A.; Warner, I. M. Nontemplated Approach to Tuning the Spectral Properties of Cyanine-Based Fluorescent NanoGUMBOS. *Langmuir* **2010**, *26* (15), 12867−12876.

(21) Li, M.; De Rooy, S. L.; Bwambok, D. K.; El-Zahab, B.; DiTusa, J. F.; Warner, I. M. Magnetic chiral ionic liquids derived from amino acids. *Chem. Commun.* **2009**, *45*, 6922−6924.

(22) de Rooy, S. L.; El-Zahab, B.; Li, M.; Das, S.; Broering, E.; Chandler, L.; Warner, I. M. Fluorescent one-dimensional nanostructures from a group of uniform materials based on organic salts. *Chem. Commun.* **2011**, *47* (31), 8916−8918.
(23) Jia, Z. Q.; Ma, Y.; Yang, W. S.; Yao, J. N. Effects of bad solvents on thiatricarbocyanine particles formation. *Colloids Surf., A* **2006**, *272* (3), 164−169.
(24) (a) Kasai, H.; Nalwa, H. S.; Oikawa, H.; Okada, S.; Matsuda, H.; Minami, N.; Kakuta, A.; Ono, K.; Mukoh, A.; Nakanishi, H. A Novel Preparation Method of Organic Microcrystals. *Jpn. J. Appl. Phys., Part 2* **1992**, *31* (8A), L1132−L1134. (b) Welton, T. Room-temperature ionic liquids. Solvents for synthesis and catalysis. *Chem. Rev.* **1999**, *99* (8), 2071−2083. (c) Kasai, H.; Yoshikawa, Y.; Seko, T.; Okada, S.; Oikawa, H.; Mastuda, H.; Watanabe, A.; Ito, O.; Toyotama, H.; Nakanishi, H. Optical properties of perylene microcrystals. *Mol. Cryst. Liq. Cryst. Sci. Technol., Sect. A* **1997**, *294*, 173−176.
(25) Faul, C. F. J.; Antonietti, M. Ionic self-assembly: Facile synthesis of supramolecular materials. *Adv. Mater.* **2003**, *15* (9), 673−683.
(26) Kasai, H.; Nalwa, H. S.; Oikawa, H.; Okada, S.; Matsuda, H.; Minami, N.; Kakuta, A.; Ono, K.; Mukoh, A.; Nakanishi, H. A Novel Preparation Method of Organic Microcrystals. *Jpn. J. Appl. Phys., Part 2* **1992**, *31* (8A), L1132−L1134.
(27) Lakowicz, J. R. *Principles of Fluorescence Spectroscopy*, 2nd ed.; Kluwer: New York, 1999.
(28) Dai, Z. F.; Dahne, L.; Donath, E.; Mohwald, H. Mimicking photosynthetic two-step energy transfer in cyanine triads assembled into capsules. *Langmuir* **2002**, *18* (12), 4553−4555.
(29) Kabatc, J.; Paczkowski, J. The photophysical and photochemical properties of the oxacarbocyanine and thiacarbocyanine dyes. *Dyes Pigm.* **2004**, *61* (1), 1−16.